Cellular Flame Instabilities

Bradley D.*, Lawes M., Mumby R.

University of Leeds, School of Mechanical Engineering, Leeds, UK
**Corresponding author email: d.bradley@leeds.ac.uk*

ABSTRACT

The onset of Darrieus Landau and thermo-diffusive instabilities in an exploding spherical laminar flame is marked by the value of the Peclet number, Pe_{cl}, which is dependent upon the Markstein number. Values of Pe_{cl} for a number of different mixtures have been measured at 0.5 and 1.0 MPa in a spherical explosion bomb. These values are presented as a function of the flame speed Markstein number, Ma_b, and it is found that neither different pressures nor the different mixtures have a great effect on this correlation. Values derived from much larger-scale atmospheric explosions of methane/air and propane/air also closely follow the same correlation. This suggests data from high pressure laboratory explosions might be used to predict the effects of large scale atmospheric explosions. Findings from other workers follow the same trend, although different detailed results can arise from both different definitions of Markstein number, and different measurement techniques.

Because of the importance of a necessary minimal stretch rate to stabilise a flame, a more logical and fundamental criterion for the onset of this type of instability is one based on the flame stretch rate, such as a critical Karlovitz stretch factor, K_{cl}. As a result, the correlations are also expressed in terms of K_{cl}, instead of Pe_{cl}. As Ma_{sr} becomes highly negative, the regime of stability is severely reduced.

KEYWORDS: Darrieus Landau, thermo-diffusive instabilities, large-scale explosions, critical Peclet number.

NOMENCLATURE

S_n	stretched flame speed (m/s)
S_s	unstretched flame speed (m/s)
u_l	unstretched laminar burning velocity (m/s)
L_b	burned gas Markstein length (m)
Ma_b	flame speed Markstein number
Ma_{sr}	burning velocity strain rate Markstein number
Pe_{cl}	critical Peclet number
K_{cl}	critical Karlovitz number
r	radius (m)
t	time (s)

Greek

α	flame stretch rate (1/s)
δ	flame thickness (m)
ν	kinematic viscosity (m^2/s)
σ	unburned to burned gas density ratio
ϕ	equivalence ratio

Subscripts

cl	critical
u	unburned
b	burned
sr	stretch rate

INTRODUCTION

As the flame radius increases in a spherical explosion flame, the flame stretch rate decreases and when it falls below a certain threshold, the Darrieus Landau and thermo-diffusive instabilities create increasingly severe wrinkling of the initially smooth laminar flame surface. As the flame radius of a spherical flame increases further, the wrinkling of its surface extends over an ever-increasing

Proceedings of the Eighth International Seminar on Fire and Explosion Hazards (ISFEH8), pp. 579-587
Edited by Chao J., Liu N. A., Molkov V., Sunderland P., Tamanini F. and Torero J.
Published by USTC Press
ISBN:978-7-312-04104-4 DOI:10.20285/c.sklfs.8thISFEH.058

range of curvatures, resulting in an increasing flame speed and a strengthening of the pressure pulse [1]. The resolution of the wrinkled surface, the derivation of its surface area and its increasing flame speed have presented severe problems in attempts to mathematically model the phenomena, and solutions have not been possible beyond a radius of a few cm. Consequently, semi-theoretical studies have involved a combination of fractal analyses [2, 3] and experiments [4, 5], some on a larger scale, extending to several metres [6-8].

A key parameter for the spherical flame is the critical flame radius, r_{cl}, that marks the onset of the unstable flame with an increasing flame speed. Because of the thermo-diffusive character of the instability, this would be expected to have a dependency upon the burning velocity strain rate Markstein number, Ma_{sr}. The appropriate dimensionless radius is the Peclet number, Pe_{cl}, comprising r_{cl}, normalised by the flame thickness, δ, equal to the cold mixture kinematic viscosity divided by the unstretched laminar burning velocity.

As a result, a key objective is to derive the flame speed, Pe_{cl}, and Ma_{sr}. If the dependency of Pe_{cl} on Ma_{sr} is independent of the pressure, then the high values of r_{cl}, that might occur in large atmospheric explosions, could be predictable from measurements in smaller, high pressure, laboratory explosions. This is because of the increase in Pe_{cl} with increased pressure due to the reduction in δ as the pressure is increased. The purpose of the present paper is therefore two fold, first, to ascertain whether the Pe_{cl}/Ma_{sr} relationship that has been reported, is valid for a range of fuels at pressures higher than atmospheric, and second, whether such relationships might predict the onset of instabilities in large atmospheric explosions.

EXPERIMENTAL TECHNIQUE

Measurements of spherical flame propagation were made in a spherical stainless steel bomb with three pairs of orthogonal windows of 150 mm diameter in [9]. The internal radius of the bomb was 190 mm. The bomb and mixture could be heated and the initial gas temperature was measured with a sheathed chromel–alumel thermocouple. Four fans, driven by electric motors, located close to the wall of the bomb initially mixed the reactants. With liquid fuels, it was vital to ensure all the liquid was evaporated and the fans enhanced heat transfer and promoted mixing. Flame speeds, together with the critical radii, r_{cl}, were measured for a variety of fuel/air mixtures, at constant pressure, by high speed ciné imaging. The onset of flame cellularity and increasing flame speed are indicative of the onset of Darrieus Landau, thermo-diffusive instabilities. The maximum possible measured flame radii, r_u, were 70 mm, set by the size of the window and increasing pressure. Pressures were 0.5 and 1.0 MPa, temperature 360 K, and equivalence ratios, ϕ, of a variety of mixtures, ranged between 0.8 and 1.3. The flame speeds, $S_n = \mathrm{d}r_u/\mathrm{d}t$, changed with the leading radius of the flame front, r_u, due to the changing flame stretch rate, given by $\alpha = (2/r_u)(\mathrm{d}r_u/\mathrm{d}t)$. Values of S_n within the stable regime were plotted against α. This relationship became more linear with increasing pressure and was extrapolated to zero stretch rate to obtain the imaginary, notional, flame speed at zero stretch rate, S_s. This enabled the Markstein length, L_b, to be obtained, from the expression.

$$S_s - S_n = L_b \alpha . \qquad (1)$$

The zero stretch rate laminar burning velocity, u_l, is given by $u_l = S_s/\sigma$, with σ the unburned/burned gas density ratio. The length, L_b, and the radius r_{cl} were both normalised by the laminar flame thickness, δ, to yield the flame speed Markstein number Ma_b and the critical Peclet number, Pe_{cl},

respectively. Fuller details of the techniques are provided in [9]. Values of σ and v were obtained using GasEq [10].

EXPERIMENTAL RESULTS AND DISCUSSION

The measured values of Pe_{cl}, at two pressures, are conveniently expressed most directly in terms of the measured values of the flame speed Ma_b, as in Figs. 1 and 2. The symbols on the lowest of the plots on each figure indicate the derived values of Pe_{cl} for a variety of fuel/air mixtures, at pressures of 0.5 and 1.0 MPa, respectively. Each experimental point is the mean from three explosions. Bearing in mind the inevitable experimental scatter in both of the measured parameters, it is striking that the influences of both the fuel and pressure are relatively small. It remains to be seen whether such small scale laboratory determinations might be a guide to Pe_{cl} values in much larger scale explosions.

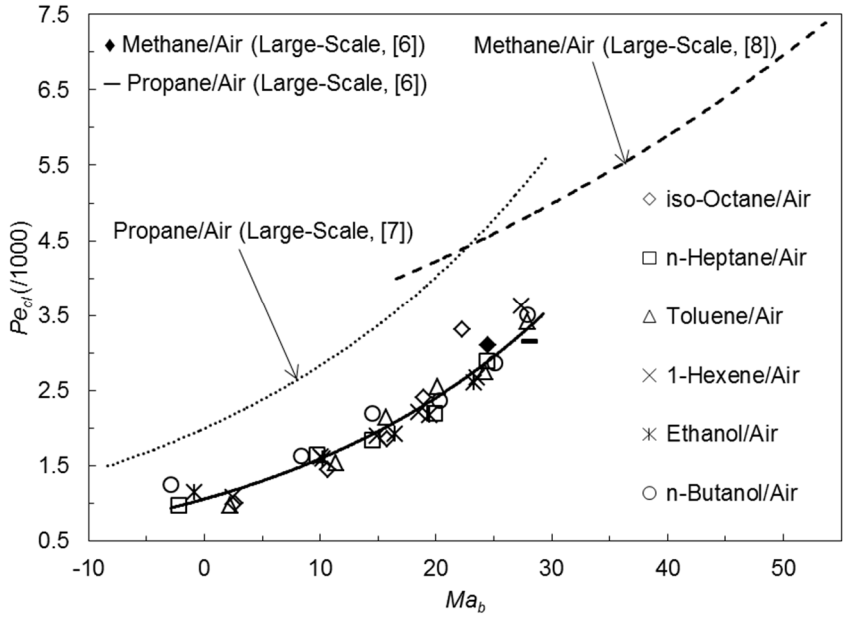

Figure 1. Pe_{cl} variation with Ma_b for different fuel/air mixtures at 0.5 MPa. Dotted curve represents correlated large scale atmospheric propane values from [7] and dashed curve large-scale atmospheric methane values from [8].

To test this possibility, on the same figure, are plotted the values from two much larger atmospheric explosions, conducted by Shell Research Ltd. in a large vented steel box structure 10 m, long, 8.75 m wide and 6.25 m high [6]. Flame speeds were measured up to a radius of 3.5 m for CH_4/air, $\phi = 1.1$, and C_3H_8/air, $\phi = 1.06$. The black diamond symbol represents the methane explosion and the black bar that of propane on the lowest plots of both figures. Bearing in mind the difference in presssure, fuels, equivalence ratios and size, there is a satisfactory correlation, at each of the two presssures, between the Pe_{cl} and Ma_b values of the many different mixtures, irrespective of their value of ϕ. Furthermore, comparison of the two figures shows but a small influence of pressure. Importantly, the two sets of coordinates from the large atmospheric explosions are close to those from the small high pressure explosions at 0.5 MPa, and slightly higher at 1.0 MPa. This suggests that instability data from high

pressure laboratory explosions might be used to predict instability effects in large scale atmospheric explosions.

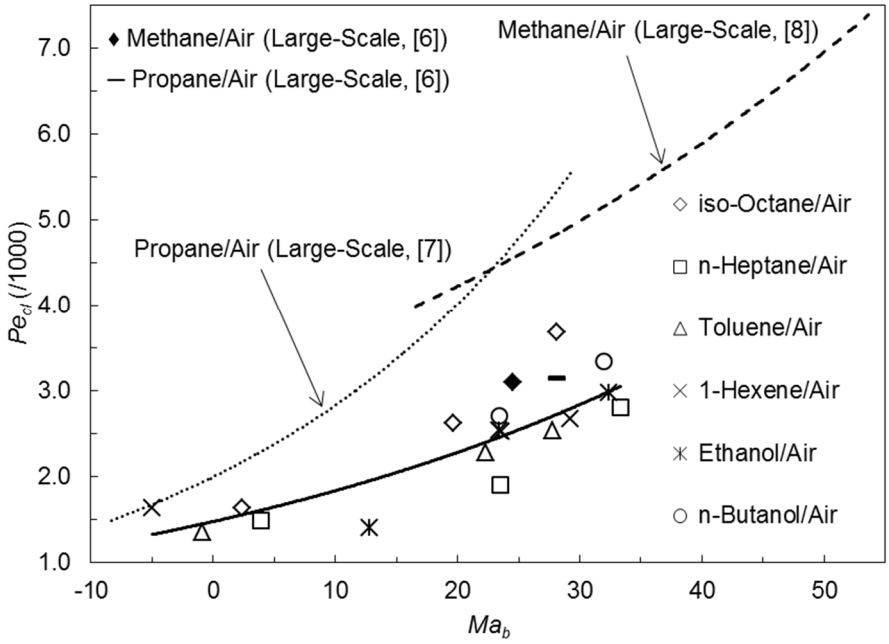

Figure 2. Pe_{cl} variation with Ma_b for different fuel/air mixtures at 1.0 MPa. Dotted curve represents correlated large scale atmospheric propane values from [7] and dashed curve large-scale atmospheric methane values from [8].

Values of Pe_{cl} also have been presented by the Factory Mutual group for large scale atmospheric explosions, in [7] for propane/air flames, and in [8] for methane/air. These flames were up to 2 m diameter, with ϕ ranging between 0.81-1.22. These values were plotted against values of Markstein numbers, taken from [11], that were numerically closer to the burning velocity strain rate Markstein numbers, Ma_{sr}, than the flame speed Markstein numbers, Ma_b [12]. To compare these values from [7] and [8] more closely with those in the present study, it was assumed that they were those of Ma_{sr}. These were then converted to Ma_b using the tabulated values of the different Markstein numbers in [5] for methane, and in [13] for propane. Necessary data for obtaining δ were taken from [10]. The numerous correlated data points from [7] and [8], after this conversion, yielded the upper broken curves, also shown in Figs. 1 and 2. The dotted curve represents propane results and the dashed curve those for methane.

There is a general consistency between these two curves, with greater stability at the higher Markstein numbers for the methane flames at both 0.5 and 1.0 MPa. As with the lower curve from the present study, the general correlation of Pe_{cl} in terms of Ma_b is confirmed. The difference between these curves and the lower one might be attributable to the different ways of defining the Markstein numbers, not only between Ma_b and Ma_{sr}, but also between the different expressions for the latter [11, 12]. Errors in its measurement are also important [11], including the extrapolation to zero stretch rate. Others might arise form the different ways in which the critical radius is measured at the onset of the instability.

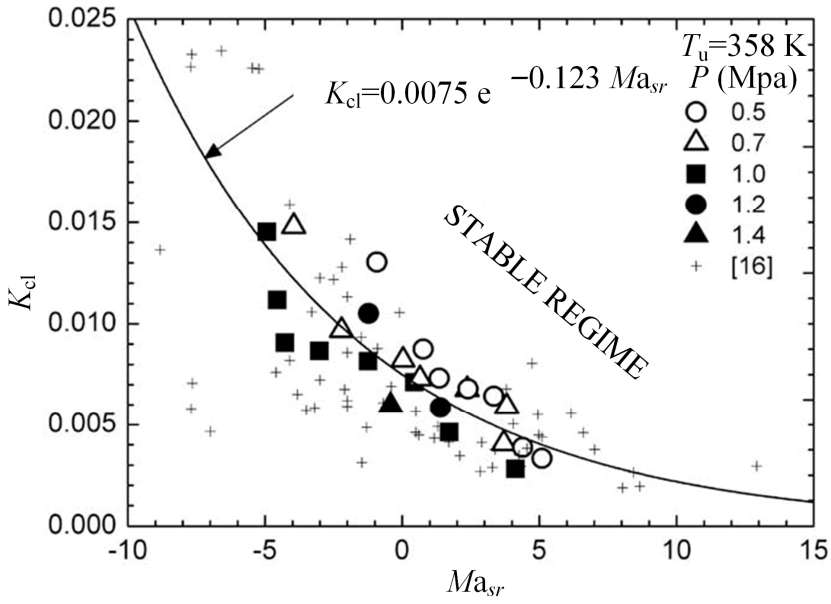

Figure 3. Values K_{cl} as a function of Ma_{sr} for ethanol/air at different pressures and ϕ from [9], expressed in terms of Ma_{sr}. Cross symbol shows data for other mixtures from [14], not [16], as indicated in the reproduced figure.

THE CRITICAL KARLOVITZ STRETCH FACTOR

That a minimal stretch rate is necessary to stabilise a flame extends beyond spherical flames and in [9] this instability criterion was expressed as a critical Karlovitz stretch factor, K_{cl}, rather than Pe_{cl}. At normalised stretch rates below K_{cl}, the flame becomes unstable. This approach is pursued in [9], where it is shown that, for a spherical premixed laminar flame:

$$K_{cl} = \left(2\sigma / Pe_{cl}\right)\left[1+(2Ma_b / Pe_{cl}\right]^{-1}. \quad (2)$$

Values of K_{cl}, as a function of $Ma_{sr,}$ are shown in Fig. 3, which is reproduced from [9]. This study was based on ethanol/air mixtures, with ϕ between 0.8 and 1.4, and the principal data points are for this fuel. Considering the wide range of pressure. indicated on Fig. 3, and range of mixtures, the single bold curve represents a satisfactory generalised correlation, although the data points on the figure that were taken from [14] are not as well correlated. It is, however, clear that, as Ma_{sr} becomes highly negative, the regime of stability is severely narrowed, while the regime of stability readily can be identified.

Values of K_{cl} also were obtained from all the data in Figs. 1 and 2, using Eq. (2), and these are re-presented in terms of $Ma_{b.}$ Fig. 4 is the counterpart of Fig. 1, and Fig. 5 that of Fig. 2. Again, the same symbols are used to represent the large scale atmospheric explosions of [6]. Also shown in Figs. 4 and 5 are transformed curves, equivalent to the broken curves that appear in Figs. 1 and 2. These show the data from the large scale explosions reported in [7] and [8].

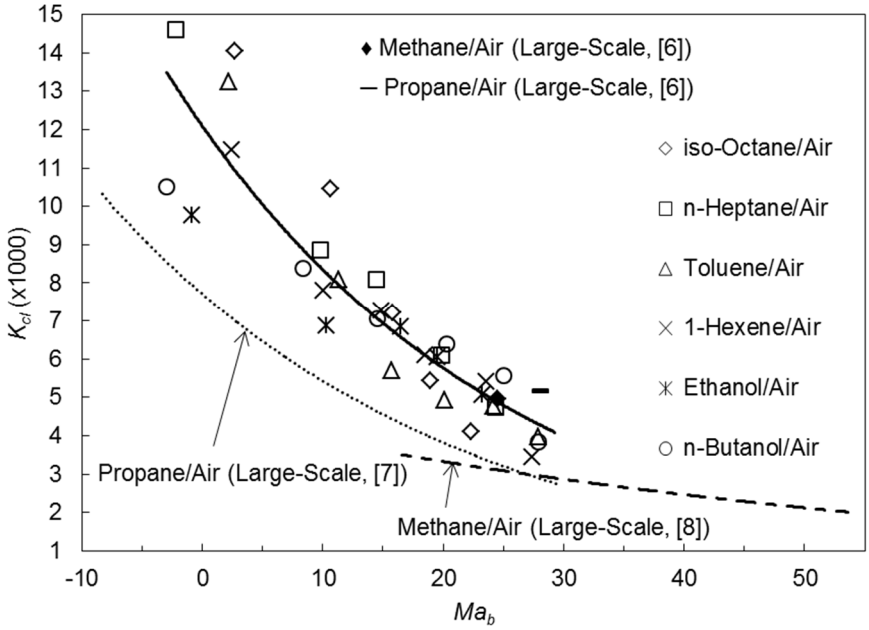

Figure 4. K_{cl} variation with Ma_b for different liquid pure fuel/air mixtures measured in the explosion bomb, at 0.5 MPa, alongside corresponding data for large-scale explosions of methane/air [6, 7] and propane/air [6, 8]. The solid black curve is the best fit through the bomb data.

Ideally, the three correlation curves on Figs. 4 and 5 would collapse into a single curve, yet there are clearly three different correlations. The probable reasons for differences between curves have been discussed in the previous Section. Different forms of Markstein number are relevant, and there can be no certainty that different research groups define Markstein numbers in the same way.

Finally, shown in Fig. 6 is another combination of data from different groups, this time expressed entirely in terms of Ma_{sr}. In this case, the high pressure ethanol/air data from explosions at elevated pressures in the same explosion bomb as that used in the current work [9], are combined with the large scale atmospheric explosion data for methane and propane from [7] and [8]. The large scale atmospheric data from [6] correlate reasonably well with the bomb data. The three correlating curves on the figure are in fairly close agreement, and again support the view that small high pressure explosions can give a fairly good indication of the onset of instabilities in very large explosions at atmospheric explosions. The developing acceleration of the flame front, after the onset of the instabilities, can give rise to appreciable pressure pulses [1].

It is interesting to note that in the correlation of normalised turbulent burning velocities in terms of the associated Karlovitz stretch factor and Ma_{sr} in [15], for $Ma_{sr} = -5$ a regime of laminar/turbulent instability is entered when the Karlovitz stretch factor becomes less than about 0.02. This compares with a value of K_{cl} of about 0.014 for $Ma_{sr} = -5$ in Fig. 6.

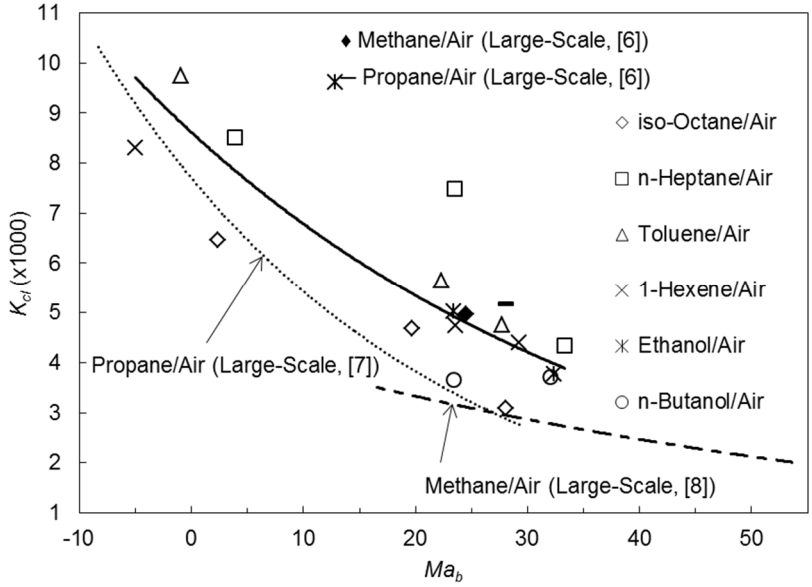

Figure 5. K_{cl} variation with Ma_b for different liquid pure fuel/air mixtures measured in the explosion bomb, at 1.0 MPa, alongside corresponding data for large-scale explosions of methane/air [6, 7] and propane/air [6, 8]. The solid black curve is the best fit through the bomb data.

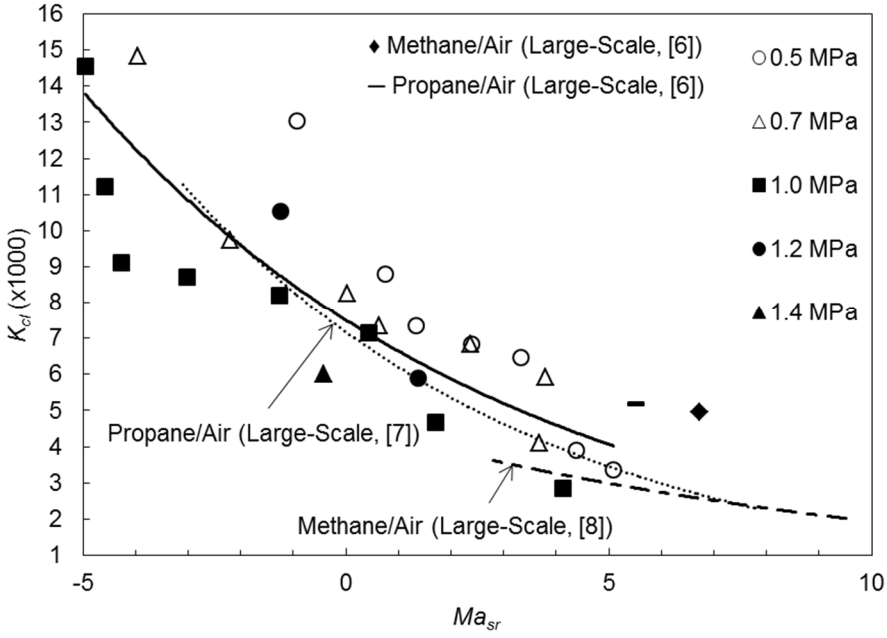

Figure 6. K_{cl} variation with Ma_{sr} for ethanol/air bomb data from Fig. 3, and large-scale atmospheric methane [6, 8] and propane [6, 7] explosions. Solid black curve shows a best fit through the bomb data.

CONCLUSIONS

Observations on the onset of Darrieus Landau and thermo-diffusive instabilities have been compared for relatively small spherical bomb explosions over a wide range of fuel/air mixtures at pressures of 0.5 and 1.0 MPa, for large explosions at atmospheric pressure. Results have been expressed as values of both the critical Peclet number at the onset of the instability, and the critical Karlovitz number, as a function of either the flame speed Markstein number, or the strain rate Markstein number. Plotted in this form, there is a fairly good correlation of the three parameters, irrespective of the fuel and the pressure. This suggests that data on the onset of instabilities from small, high pressure, laboratory explosions might be used to predict their onset in large scale atmospheric explosions. A prime cause of scatter in the correlation would appear to arise from Markstein number uncertainties.

ACKNOWLEDGEMENT

EPSRC is thanked for the Award of a Research Scholarship to Richard Mumby.

REFERENCES

1. Bradley, D., Dowling, A. P., and Morgans, A. S. Combustion Instabilities, In: Turbulent Premixed Flames, Swaminathan, N. and Bray, K. N. C. (eds.), Cambridge University Press, pp. 151-243, 2011.
2. Gostintsev, Y. A., Istratov, A. G., and Shulenin, Yu. V. Self-similar Propagation of a Free Turbulent Flame in Mixed Gas Mixtures, Combustion, Explosion and Shock Waves, 24(5): 563-569, 1988.
3. Bradley, D. Instabilities and Flame Speeds in Large-Scale Premixed Gaseous Explosions, Philosophical Transactions of the Royal Society of London A: Mathematical, Physical and Engineering Sciences, 357(1764): 3567-3581, 1999.
4. Bradley, D., Hicks, R. A., Lawes, M., Sheppard, C. G. W., and Woolley, R. The Measurement of Laminar Burning Velocities and Markstein Numbers for ISO-Octane-Air and ISO-Ooctane-*n*-Heptane-Air Mixtures at Elevated Temperatures and Pressures in an Explosion Bomb, Combustion and Flame, 115(1): 126-144, 1998.
5. Gu, X. J., Haq, M. Z., Lawes, M., and Woolley, R. Laminar Burning Velocity and Markstein Lengths of Methane-Air Mixtures, Combustion and Flame, 121(1): 41-58, 2000.
6. Bradley, D., Cresswell, T. M., and Puttock, J. S. Flame Acceleration Due to Flame-Induced Instabilities in Large-Scale Explosions, Combustion and Flame, 124(4): 551-559, 2001.
7. Bauwens, C. R., Bergthorson, J. M., and Dorofeev, S. B. Experimental Study of Spherical-Flame Acceleration Mechanisms in Large-Scale Propane-Air Flames, Proceedings of the Combustion Institute, 35(2): 2059-2066, 2015.
8. Bauwens, C. R., Bergthorson, J. M., and Dorofeev, S. B. Critical Peclet Numbers for the Onset of Darrieus-Landau Instability in Atmospheric-Pressure Methane-Air Flames, 25th International Colloquium on the Dynamics of Explosions and Reactive Systems, Leeds, UK, 2015.
9. Bradley, D., Lawes, M., and Mansour, M. S. Explosion Bomb Measurements of Ethanol-Air Laminar Gaseous Flame Characteristics, at Pressures up to 1.4 MPa, Combustion and Flame, 156(7): 1462-1470, 2009.
10. Morley, C. Gaseq: A Chemical Equilibrium Program for Windows, http://www.gaseq.co.uk, 2005.
11. Taylor, S. C. Burning Velocity and the Influence of Flame Stretch, PhD Thesis, University of Leeds, 1991.
12. Bradley, D., Gaskell, P. H., and Gu, X. J. Burning Velocities, Markstein Lengths, and Flame Quenching for Spherical Methane-Air Flames: A Computational Study, Combustion and Flame, 104(1-2): 176-198, 1996.
13. Bradley, D., Gaskell, P. H., and Gu, X. J. The Modelling of Aerodynamic Strain Rate and Flame Curvature Effects in Premixed Turbulent Combustion, Proceedings of the Combustion Institute, 27(1): 849-856, 1998.

14. Bradley, D., Lawes, M., and Liu, K. Limiting Flame Stretch Rates for Flame Instabilities and Flame Quenching, In: Proceedings of the Fifth International Seminar on Fire and Explosion Hazards, Bradley, D., Drysdale, D. and Molkov, V. (eds.), University of Edinburgh, pp. 634-643, 2008.
15. Bradley, D., Lawes, M., Liu, K. X., and Mansour, M. S. Measurements and Correlations of Turbulent Burning Velocities over Wide Ranges of Fuels and Elevated Pressures, Proceedings of the Combustion Institute, 34(1): 1519-1526, 2013.